

# Electron paramagnetic resonance analysis of the vimentin tail domain reveals points of order in a largely disordered region and conformational adaptation upon filament assembly

John F. Hess,<sup>1</sup> Madhu S. Budamagunta,<sup>2</sup> Atya Aziz,<sup>1</sup> Paul G. FitzGerald,<sup>1\*</sup> and John C. Voss<sup>2</sup>

<sup>1</sup>Department of Cell Biology and Human Anatomy, University of California, Davis, California 95616

<sup>2</sup>Department of Biochemistry and Molecular Medicine, University of California, Davis, California 95616

Received 29 June 2012; Accepted 15 October 2012

DOI: 10.1002/pro.2182

Published online 25 October 2012 proteinscience.org

**Abstract:** Very little data have been reported that describe the structure of the tail domain of any cytoplasmic intermediate filament (IF) protein. We report here the results of studies using site directed spin labeling and electron paramagnetic resonance (SDSL-EPR) to explore the structure and dynamics of the tail domain of human vimentin in tetramers (protofilaments) and filaments. The data demonstrate that in contrast to the vimentin head and rod domains, the tail domains are not closely apposed in protofilaments. However, upon assembly into intact IFs, several sites, including positions 445, 446, 451, and 452, the conserved “beta-site,” become closely apposed, indicating dynamic changes in tail domain structure that accompany filament elongation. No evidence is seen for coiled-coil structure within the region studied, in either protofilaments or assembled filaments. EPR analysis also establishes that more than half of the tail domain is very flexible in both the assembly intermediate and the intact IF. However, by positioning the spin label at distinct sites, EPR is able to identify both the rod proximal region and sites flanking the beta-site motif as rigid locations within the tail. The rod proximal region is well assembled at the tetramer stage with only slight changes occurring during filament elongation. In contrast, at the beta site, the polypeptide backbone transitions from flexible in the assembly intermediate to much more rigid in the intact IF. These data support a model in which the distal tail domain structure undergoes significant conformational change during filament elongation and final assembly.

**Keywords:** vimentin; intermediate filaments; site-directed spin labeling; electron paramagnetic resonance

---

*Abbreviations:* CC, coiled-coil; EPR, electron paramagnetic resonance; HIM, helix initiation motif; HTM, helix termination motif; IF, intermediate filament; NMR, nuclear magnetic resonance; SDSL-EPR, site directed spin labeling-electron paramagnetic resonance.

Additional Supporting Information may be found in the online version of this article.

Grant sponsor: National Institutes of Health; Grant number: EY015560; Grant sponsor: NEI Core Facilities; Grant numbers: P30-EY012576, AG029246; Grant sponsor: Research Facilities Improvement Program from National Center for Research Resources, National Institutes of Health; Grant number: C06 RR-12088-01.

\*Correspondence to: Paul G. FitzGerald, Department of Cell Biology and Human Anatomy, University of California, 1 Shields Ave, Davis, CA 95616. E-mail: pgfitzgerald@ucdavis.edu

## Introduction

There are more than 65 different proteins used in the assembly of human intermediate filaments (IFs), and IF proteins represent one of the most abundant of cellular proteins.<sup>1</sup> Mutations in IF genes have been implicated in at least 85 different human diseases, encompassing skin blistering disorders due to keratins mutations, muscular dystrophies due to mutations in desmin, and accelerated aging syndromes (and other syndromes) due to mutations in lamins.<sup>2</sup> In terms of inherited disorders, the Type III intermediate filament protein vimentin, one of the best-conserved IF proteins, seems atypical; the original mouse knock out was proclaimed to be without a detectable phenotype,<sup>3</sup> though recently a human vimentin mutation has been linked to cataracts.<sup>4</sup> However, despite abundance and pathogenic impact of IF protein mutations, no IF or IF proteins has been successfully crystallized, thus we lack a complete structure for any IF or IF protein. As a consequence, we lack a mechanistic understanding of normal IF function. Sequence analysis suggests that IF proteins share a conserved predicted secondary structure dominated by a central rod domain, flanked by head and tail domains.<sup>5–10</sup> Though there is considerable sequence variation in IF rod domains, analysis predicts that all IF central rod domains form coiled-coil dimers.<sup>11–13</sup> In recent years, crystallography of vimentin IF rod domain fragments and site directed spin labeling and electron paramagnetic resonance (SDSL-EPR) of vimentin IFs under physiologic conditions have provided substantial evidence that supports some aspects of the structure of the central rod domain while forcing a revision of other aspects.<sup>14–22</sup> SDSL-EPR is a spectroscopic technique that measures the behavior of a small, amino acid-sized, nitroxide spin label covalently attached to an introduced cysteine to provide structural information about that precise position of the protein. Using simple mutagenesis techniques, a cysteine residue can be positioned sequentially at any (or every) location in a protein chain (while leaving the remaining peptide sequence unchanged) and a spin label coupled to that cysteine. Incubation of the labeled protein in different conditions then provides structural information about (1) the peptide backbone flexibility and (2) the proximity between spin labels at specific locations in the range of 0–2.1 nm. Throughout our experiments we have found vimentin to be remarkably tolerant of the introduced spin label, in most cases assembling into native appearing 10 nm filaments. Because SDSL-EPR provides structural data near the spin-labeled site, overall structure is deduced by placing a series of spin labels along the polypeptide backbone, and subsequently assembling these “snapshots” into a larger montage of regional structure.

Mutagenesis and *in vitro* assembly studies have been used to assess the importance of the head and

tail domains in the process of IF assembly.<sup>23–30</sup> However, there had been very little data generated which identify structure in either head or tail<sup>31,32</sup> until the recent report by Aziz *et al.*, who used SDSL-EPR to generate data that describes structure in the vimentin head domain.<sup>15</sup> Based on deletion mutagenesis and *in vitro* assembly studies, it is generally agreed that the head domain is more important for IF assembly than the tail domain; deletion of the head domain interrupts filament assembly at the dimer/tetramer stage.<sup>28,29</sup> In contrast, several published reports demonstrate assembly of tail-less vimentin molecules while other reports found that tail mutants formed IFs with subtle differences from the wild type.<sup>24,27,28,33–35</sup> A study of the interaction between the isolated vimentin tail domain and actin-containing structures suggested that the vimentin tail existed mainly in an extended conformation.<sup>31</sup> Computerized predictions of vimentin tail structure reveal predominantly extended strand and random coil structure.

Early in the cloning and sequence determination of IFs, amino acid sequence comparisons identified a sequence motif in the tail that is conserved between desmin, vimentin, and peripherin: TRDG. Glial fibrillary acidic protein (GFAP), a Type III IF protein like vimentin, contains a slight variant: MRDG.<sup>36</sup> This sequence was predicted to form a beta turn, hence the name “beta site”<sup>25</sup> and was subsequently identified as a region important for the correct assembly of 10 nm filaments.<sup>24,37</sup> Additional studies by Herrmann *et al.* identified mass per length differences between IFs assembled from wild type or tail-mutated proteins,<sup>28</sup> the general conclusion being that the tail domain was at least partially responsible for proper filament diameter.

We recently reported the results of SDSL-EPR analysis of the head domain of vimentin, demonstrating that the two domains travel in parallel, in close proximity over their entire length, and that they fold back onto the rod domain, imparting an unexpected sidedness to the vimentin dimer.<sup>14,15</sup> In this report, we take an analogous approach to the study of the vimentin tail domain. Our data show that the head and tail domains of vimentin are structurally very different and the tail domain undergoes distinctive conformational change upon assembly from tetrameric protofilament to mature filament.

## Results

### **Tail domain spectra collected from tetramers**

A model of vimentin structure is shown in Figure 1. The crystal structure of the end of the rod domain led to the deduction that coiled-coil structure terminates with glu<sup>405</sup>.<sup>21</sup> The tail domain contains two

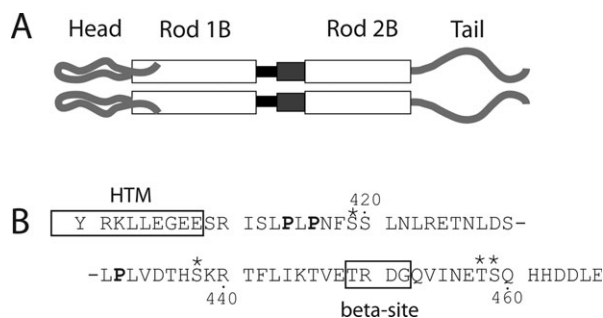


**Figure 1.** Schematic of vimentin molecular structure. Panel (A) shows a representation of the protein domains of vimentin. At the amino terminus is the head domain, leading into rod domain 1. The black box between rod 1B and rod 2B represents Linker 1–2. The dark gray box between rod 1B and rod 2B represents the parallel helices structure of rod 2A/Linker 2. Panel (B) shows the amino acid sequence of the tail domain, beginning with Y<sup>400</sup>. The HTM and  $\beta$  (beta) sites are boxed and labeled. Prolines are in bold; phosphorylation sites are indicated by asterisks.

highly conserved motifs: (1) the “helix termination motif” (HTM) spanning residues 399–408, found at the predicted end of the rod domain and (2) the beta-site motif at residues 446–454. The beta-site motif (human vimentin TVETRDGQV) was named on the basis of a beta turn predicted to occur at the amino acid sequence T<sup>449</sup>RGD<sup>452</sup> and has been implicated in the proper regulation of IF diameter in Type III homopolymeric proteins.<sup>24,25,28,38</sup>

SDSL-EPR analysis of vimentin tail structure began with collection of spectra from samples in 5 mM Tris, pH 7.5, conditions that permit assembly of tetramers<sup>39</sup> (also known as protofilaments; a molecular building block that rapidly assembles upon addition of salt). SDSL-EPR was performed at positions beginning with Arg<sup>401</sup>, continuing to Thr<sup>458</sup>, although not every position was assayed (see Fig. 2). Immediately apparent from the tetrameric protofilament spectra shown in Figure 2 is the extremely broadened spectra from spin labels located at positions 401–410. These spectra have been amplified by a factor of 4 to assist in viewing spectral line shapes. However, while the EPR spectra from this region reflect a very tightly packed structure, there is not the characteristic modulation of the spectral broadening that we observe for coiled-coiled segments. Most remarkable are positions E<sup>407</sup>, E<sup>408</sup>, and S<sup>409</sup>, in which the extreme broadening demonstrates that each position is tightly associated with its counterpart in the adjacent chain. Furthermore, the broadening of positions 407–409 is substantially stronger than is observed for sites occupying the coiled-coil interface (i.e., positions *a* and *d* in the heptad repeat). In fact, the spectra of position 407 rivals any previously obtained vimentin spectra for rigidity and represents a dramatic change from the spectra of position 406. Beyond position 410, spin labels

attached to vimentin remain in close proximity to the residues in the neighboring chain through position 416. However, a very interesting trend is evident that describes the tail domain in general: increasing mobility and decreasing proximity of adjacent chains as the spin label is positioned closer to the carboxy terminus. In fact, beyond position 420 the consistent isotropic shape of the EPR spectra indicate a lack of fixed secondary structure for the terminal 40 amino acids.

### Tail domain structure in filaments

In fully assembled filaments, spectra from spin labels placed in the highly conserved region comprised of positions 401–410 (which includes the (TY)R<sup>401</sup>KLLE-GEE motif) show no significant differences from the spectra seen in protofilaments: these spectra show a high degree of broadening, consistent with tightly associated polypeptide chains running in parallel, suggesting no major changes in structure at the end of the rod domain upon assembly (Figure 3). There is no apparent modulation of the broadening to reflect a coiled-coil structure.<sup>16–18</sup> There is no evidence to suggest the chains separate within this region.

The first notable change in the EPR spectra upon IF assembly is found at position 412, which

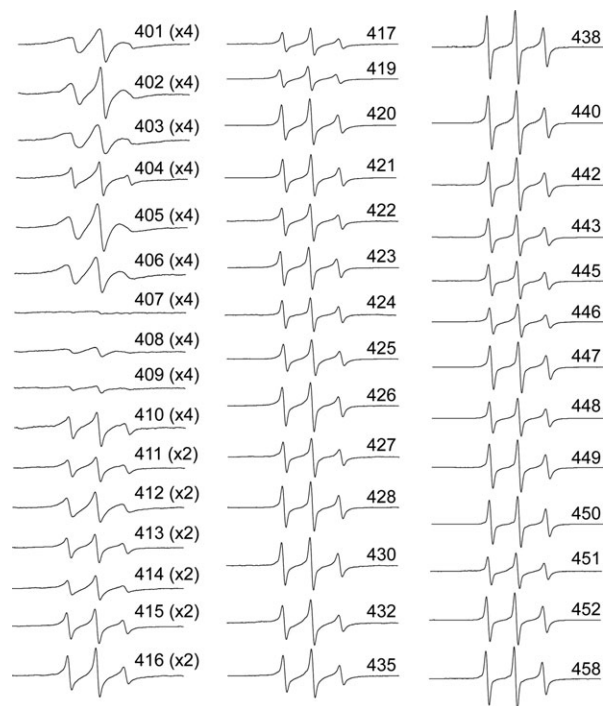


**Figure 2.** EPR spectra collected from protofilaments at room temperature (25°C). Each individually spin labeled vimentin mutant was dialyzed against low ionic strength Tris and EPR spectra collected. The data presented are all normalized as described in the materials and methods. The spectra of regions with extreme broadening (401 through 416) have been amplified by factors of 2 or 4 to provide improved resolution.

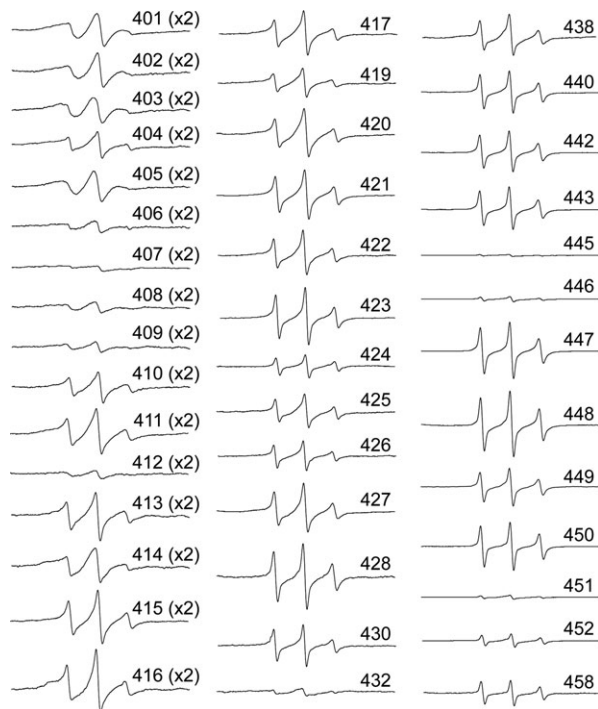


**Figure 3.** EPR spectra collected from filaments at room temperature (25°C). Each individually spin labeled vimentin mutant was dialyzed against low ionic strength tris and the appropriate volume of 10× IFAB (see methods) added immediately prior to insertion of sample into a capillary. Following a 1-h incubation, EPR spectra were collected. The data presented are all normalized as described in the materials and methods. The spectra of regions with extreme broadening (401 through 416) have been amplified by factors of 2 or 4 to provide improved resolution.

shows a substantial increase in the spin coupling. This difference indicates a closer association of spin labels at this position in the filament, and most likely a restriction of side chain dynamics as well. Based on the predicted heptad repeat pattern, position 411 could have been argued as the last heptad  $\alpha$  position of the vimentin central rod domain. However, while the spectrum of position 411 is broad relative to most of the tail region, it is less broad than its flanking residues, which is not consistent with our previous observation of interface sites within coiled-coil structure. Therefore, based on spectroscopy, we again conclude residues 401–411 are not part of the coiled-coil central rod domain.

The next few spectra (413–420) show an ordered, though not tightly packed structure, and one which also does not emulate what has been described for coiled-coil regions. From position 421 to the end of the tail however, the spectra are all indicative of a weakly ordered domain. In general, spectra from positions 421 to the end of the vimentin protein reveal a degree of backbone flexibility we have previously not seen in either the head or rod domains. Some exceptions exist, and these are discussed below.

### Structural changes upon IF formation

Spin labeled positions 412, 416, 420, 432, and 445 each show a substantial line shape difference between the two assembly states. Figure 4 presents the tetrameric protofilament and IF spectra of these positions plotted together for ease of comparison. Each position shows a considerable structural change that accompanies the assembly into IFs. In general, these line shape changes, coupled with the broadening parameters, show that these tail domain positions adopt a more structured and closely packed environment upon IF assembly.

Position 412 lies just downstream from the highly conserved TYRKLLEGEE<sup>408</sup>, and close to pro<sup>414</sup> and pro<sup>416</sup>, which would be expected to bend the polypeptide chains. The EPR spectra of 412 in low-salt shows moderate flexibility of the spin-labeled side chain, but an extremely broadened spectrum is obtained when the protein is assembled into filaments. This extreme broadening indicates a strong dipolar component in addition to any immobilization occurring, revealing that assembly results in a very close apposition of side chains located at position 412 of vimentin.

The spectra of position 420 also show a dramatic change from tetramer to IF. The backbone at this site shifts from a very mobile state as reflected by its sharp EPR spectrum in low-salt conditions, to a more ordered and closely packed state upon IF formation. Position 432, the location of the third and final proline residue within the vimentin tail, experiences stronger dipolar interaction in assembled filaments, reflecting a direct association of side chain structure at this position upon IF formation. This change in structural order and proximity is even more pronounced at position 445, which is located at the approximate beginning of the “beta site.”<sup>24,25</sup> In the protofilament state, the EPR spectrum of position 445 resembles a denatured protein, exhibiting a very high level of backbone mobility. However, upon IF formation this spectrum essentially flattens (note scaling adjustments) due to extreme dipolar coupling. Of the sites examined, position 445 displays the most extreme increase in broadening upon IF formation of the more than 150 sites we have examined (previously published data). The EPR spectrum of position 445 obtained from proto-filaments in low-salt buffer resembles urea-denatured spectra, while the spectra obtained from assembled IF samples reveal both extremely rigid protein structure and spin–spin interaction due to proximity (see below).

In contrast, the prolines located at positions 414 and 416 show an increase in the population of strongly immobilized side chains (note amplitude of broad shoulder in low-field peak, see arrow in Fig. 4), however this is not accompanied by an increase in dipolar coupling, as will be shown below. Although IF assembly increases the structural order

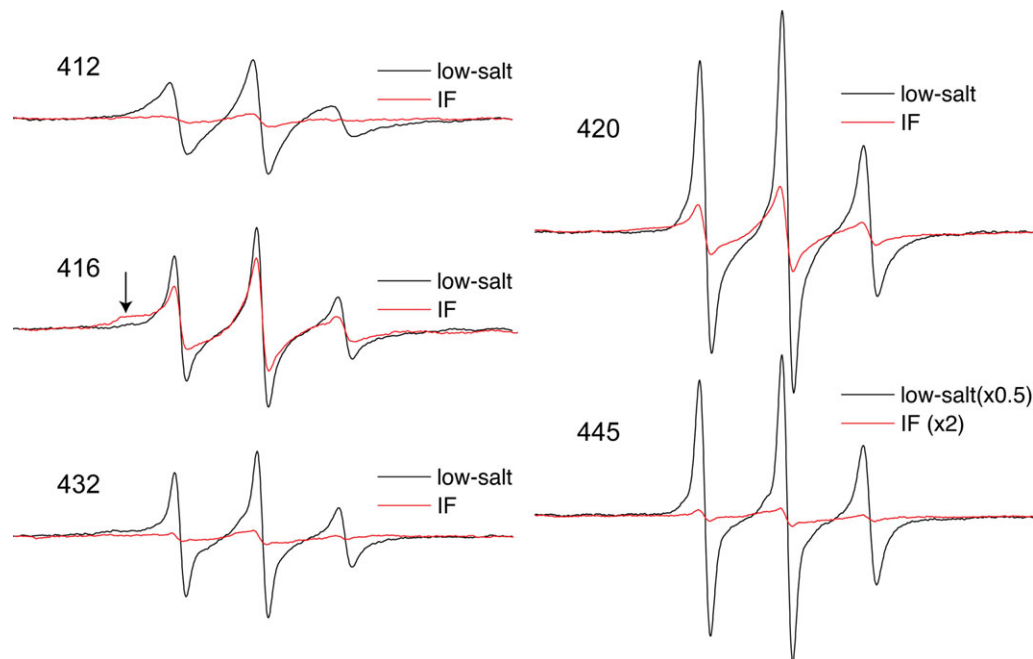


**Figure 4.** Room temperature EPR spectra of selected mutants exhibiting notable changes upon filament assembly. Protofilament and filament EPR spectra of each mutant 412, 416, 420, 432, and 445 are plotted on the same axis. Due to the magnitude of change that occurs at position 445, the amplitude of its protofilament spectrum has been halved, whereas the amplitude of the IF spectrum has been doubled for the purpose of improved IF spectrum presentation. Filament assembly induces a strong restriction in chain mobility at position 416, as evident with the broad shoulder in the low field peak (see arrow).

at positions 414 and 416, the distance between labels at these locales actually increases with IF assembly. Thus, the two prolines in this region of vimentin, while becoming more constrained in the IF state, may facilitate a splaying of the chains to accommodate packing within the macromolecular state, perhaps suggestive of lateral interactions with adjacent dimers.

In summary, most positions show an increase in order upon filament assembly, although the increase is much more dramatic at some sites (e.g., 412, 432, 445). In general, the decrease in order is accompanied by a closer packing of the spin labels within the homodimer (resulting in spin-coupling interaction, see below), with the exception of the region containing prolines 414 and 416.

#### **Relative order and proximity throughout the tail domain in both protofilaments and filaments**

A room temperature spectrum from a homogeneous sample is still potentially ambiguous due to the spectral broadening that can arise from either the close proximity of spin labels, or the loss of motional averaging with strongly immobilized spin labels within the protein structure. One way to distinguish the contributions of each broadening mechanism, is to observe all samples in the absence of motion (i.e., the frozen state), where the appearance of broadening can then be ascribed to dipolar coupling alone. We therefore collected spectra from samples frozen

at  $-100^{\circ}\text{C}$  and calculated the  $d_1/d$  values as in prior studies.<sup>14,15,18</sup> The  $d_1/d$  value is a semi-quantitative measure of the distance between spin labels, with larger values ( $>0.35$ ) reflecting proximity within 2 nm. Our calculations of  $d_1/d$  values from spectra obtained from frozen samples provide an index of broadening in the frozen state. When comparing the relative proximity of positions in the tetramer and IF assemblies, it is clear that in the frozen state both forms of vimentin share the same general trend in the  $d_1/d$  parameter [Fig. 5(A)]. The  $d_1/d$  values calculated for vimentin protofilaments clearly show the trend of lower  $d_1/d$  values as the spin label is placed closer to the carboxy terminus. Values calculated from assembled IF samples display a similar trend, but with several significant exceptions, notably 430, 432, 445, 446, 451, 452, and 458. Therefore, these sites undergo a conformational change upon IF assembly, which for each position involves a closer packing with the same position in the partner chain. While the broadening is generally greater throughout assembled vimentin (consistent with the notion of a more ordered and tightly packed tail domain upon filament assembly), the positions noted above serve as especially useful markers of assembly given the magnitude of their change.

The second moment ( $\langle H^2 \rangle$ ) of the EPR spectrum provides a semi-empirical parameter that calculates the mean-squared spectral breadth. Its numerical value increases as the frequency of spin label motion

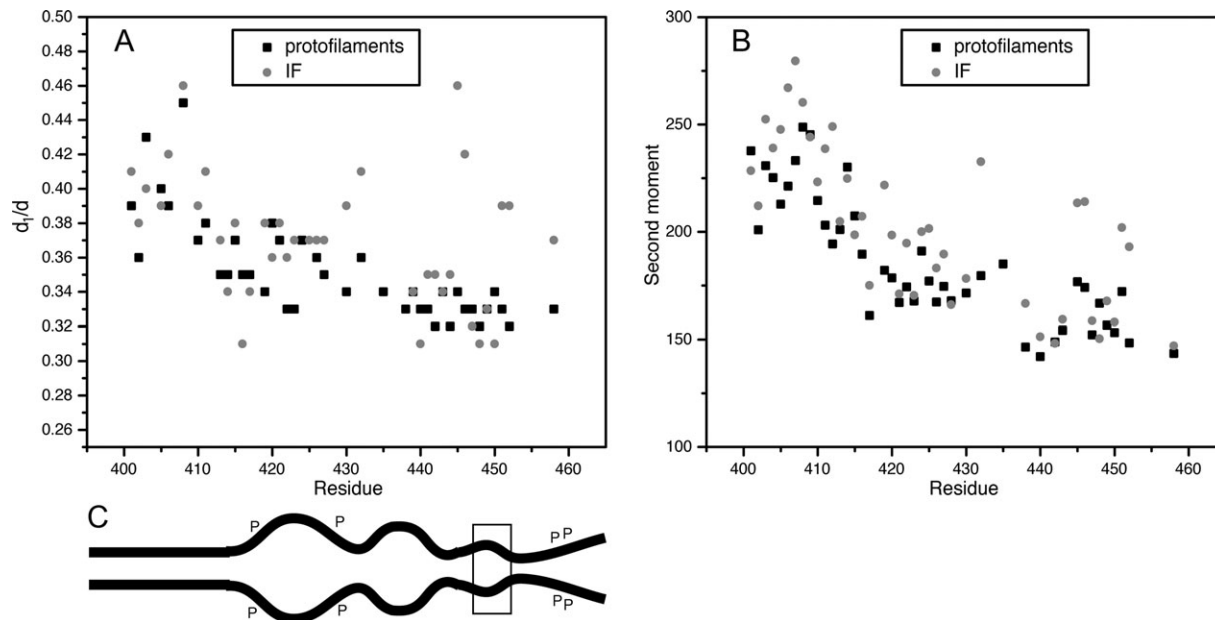


**Figure 5.** Relative order throughout the tail domain of vimentin in the protofilament and filament states. A: Plot of the motion-independent line broadening ( $d_1/d$ ) versus sequence position for frozen vimentin ( $-100^\circ\text{C}$ ). B: The spectral breadth of samples at room-temperature calculated from the spectral second moments  $\langle H^2 \rangle$  versus tail domain sequence position. Values for  $d_1/d$  and  $\langle H^2 \rangle$  data points, filament assembly and wild type amino acid identity are available in Supporting Information Table 1. C: Schematic of vimentin displaying the end of the rod domain and tail domain. The increase and decrease in distance between tails in a dimer is depicted, and correlates with the data in graph (A). “P” represents sites of phosphorylation, while the box encompasses the beta site.

is reduced. While the second moment will also be affected by broadening induced by strong dipolar coupling, smaller values of  $\langle H^2 \rangle$  are a clear indication of low structural order (fast spin label motion).<sup>40</sup> Thus, room-temperature spectra can be used to compare the relative order of the tail domains in both the tetramer and IF states of vimentin. Figure 5(B) shows a plot of the spectral second moment as a function of sequence position, providing a quantitative index of the increasing disorder as the spin label is placed progressively closer to the tail (numerical values listed in Supporting Information Table 1). Thus, the general trend displayed in this panel is from a region of more ordered structure close to the rod domain to a region with very little structural organization at the end of the tail. With respect to the low-salt samples (black boxes) only a few values violate the pattern, and they represent small deviations. More interesting are the more significant deviations from this general trend identified by data from assembled IFs (gray circles). In particular, residues 432 and several between 445 and 455 show dramatic increases in second moment values, indicating attainment of ordered secondary structure during the assembly of IFs from protofilaments. Based on these second moment calculations, the majority of positions in the tail follow the general trend of having less and less well ordered structure toward the end of the tail. Collectively, these data demonstrate that the tail

domain is not a fixed structure, but undergoes considerable change during the process of assembly.

## Discussion

We have presented SDSL-EPR data to characterize the structure and assembly of the carboxy terminal “tail” domain of vimentin, a Type III homopolymeric IF protein. Spectra were collected from spin labeled, full length recombinant human vimentin in two buffer conditions and thus different assembly states. First, in low ionic strength tris (5 mM Tris, pH 7.5), vimentin assembles into a tetrameric species<sup>39</sup> (sometimes known as protofilaments), remains highly soluble and assembles into long filaments upon the addition of salt. Second, spectra were collected from polymerized filament samples in  $1\times$  filament assembly buffer. Spectroscopic data demonstrate that the structure of the vimentin tail domain is more heterogeneous than any region of vimentin we have previously characterized. Overall, the tail domain is more flexible than the head or central rod domains (either “linker” or coiled-coil domains). In some regards, the tail domain could be functionally considered bipartite. The first third of the tail (400–420) structurally represents a continuation of the central rod domain, not as a coiled coil, but as a rigid, well-ordered end to the rod domain. This rigid, well-ordered, rod proximal tail region abruptly transitions to the remaining two-thirds of the tail (421–458), composed of a more flexible, less

ordered region. Spectroscopic data also demonstrate a different mode of assembly for this distal tail region. In general, EPR spectra from positions 421–458 show a degree of freedom that has not been observed in other regions and this freedom is retained in the assembled filament. However, spectra from several samples in this tail distal region exhibit a high degree of mobility in low-salt and greatly reduced freedom in the IF. We conclude that these positions in the tail domain are involved in protein/protein interactions that occur during filament elongation, interactions that result in a loss of mobility with the assumption of structure.

Our data on the assembly of the head domain in a previous report<sup>15</sup> and the tail in this report show a distinction from early NMR results obtained from keratins.<sup>32</sup> In the keratin experiments, isotopically labeled serine or glycine were used to label keratin proteins. Due to the abundance of these amino acids in the head and tail domains, NMR chemical shifts were interpreted as evidence of the head and tail domain structure. With this approach, Mack *et al.* concluded that the glycine/serine end domains of epidermal keratin IFs have little or no structural order in assembled filaments.<sup>32</sup> With our SDSL-EPR approach, we have been able to show that the rod proximal region, 401–420 and the entire head domain of vimentin assemble at a similar rate as the rod domain.<sup>15</sup> Our data indicate that within vimentin, it is the region 421–458 that exhibits little structural order.

The past decade has seen the publication of a number of X-ray crystallographic structures of cytoplasmic IF fragments.<sup>19,21,41–43</sup> Unfortunately, no atomic structures have been presented for the head or tail domains of cytoplasmic IFs. The recently solved structure of a nuclear lamin rod 2 fragment suggests a dual assembly role for amino acid sequences in the conserved TYRKLEGE helix termination domain but yields no structural data for the downstream tail domain.<sup>44</sup>

The spectroscopic data from the rod proximal tail reveal a lack of coiled-coil structure from vimentin positions 401–411, although  $d_1/d$  calculations suggest that the peptide chains run in parallel. Our  $d_1/d$  calculations also suggest proximity between spin labels that would not be compatible with the residues 406–409 separating and folding back as suggested by crystallography data.<sup>21,41</sup>

Our spectroscopic results are consistent with mutagenesis experiments in identifying the beta-site as structurally important. Kouklis *et al.* identified a single amino acid change, G450V and an internal deletion of 444–452 that each resulted in the assembly of irregular fibrils with a propensity to laterally aggregate.<sup>24</sup> Rogers *et al.* made a series of deletions of the *Xenopus* tail and found that the first deletion, removing the last 11 amino acids of the tail (CA11),

including the RDG sequence (beta site homology region), resulted in a protein with slightly altered assembly characteristics.<sup>27</sup> Our SDSL-EPR data reveal that within the distal tail, positions 445, 446, 451, and 452 undergo a significant structural change during the assembly of IFs from protofilaments but the mechanism by which this region contributes to the formation of consistent diameter IFs is not known. It is interesting that the beta site is flanked on each side by sites of phosphorylation, positions S<sup>430</sup>, T<sup>458</sup>, and S<sup>459</sup> that influence assembly and disassembly.<sup>45</sup>

With this spectroscopic evaluation of the vimentin tail, the structure of the fundamental building block of cytoplasmic IFs is becoming clearer. As we previously published, the head domains assemble in the same general time frame as the rod domains, and like the rods, assemble as a pair. We have identified an interaction between the head and the rod1A domain, which indicates a folding of the head back on the rod. Coiled-coils and parallel helices dominate the central rod domain again reflecting a pair-wise association of peptide chains. At the end of the rod, we find a tight association of the peptide chains with a separation occurring at about vimentin position 420. Downstream from this region, the tail domain ceases to assemble in the dimeric fashion of the rest of the molecule. It is only as the filaments elongate that the tail domains assemble. The data produced by spectroscopy do not allow for X-ray crystallographic level resolution of structure, but as in the recent past, a combination of both techniques should ultimately reveal the molecular structure of the fundamental vimentin building block.

## Materials and Methods

### Spin labeled proteins

Mutagenesis, over-expression, purification, and spin labeling were done as described in our previous reports.<sup>18</sup> In brief, spin labeled mutants were produced by substituting a cysteine residue at a series of different sites in the human vimentin tail region using mutagenic oligonucleotides and iProof polymerase (Bio-Rad, Richmond, CA). Sequence changes were verified by DNA sequencing (Davis Sequencing, Davis, CA). Between human vimentin positions 401–458, a total of 45 individual mutants were constructed. Mutant vimentin proteins were produced by bacterial over-expression. Inclusion bodies were purified using lysozyme/DNase, and sequential high/low salt washes. Isolated inclusion bodies were dissolved in 8M urea buffers and further purified by gel filtration and ion-exchange chromatography, using a GE Healthcare AKTA FPLC system (GE Healthcare, Piscataway, NJ). Following purification, a nitroxide spin label was attached to the cysteine residue by treating the purified protein with 100  $\mu$ M

TCEP (tris-(2-carboxyethyl) phosphine, hydrochloride; Life Technologies, Eugene, OR) followed by spin labeling with 500  $\mu\text{M}$  ((1-oxyl-2,2,5,5-tetramethyl-3-pyrroline-3-methyl) methanethiosulfonate (MTS-SL, Toronto Research Chemicals, Toronto, Canada). The unincorporated label was separated from spin-labeled protein by chromatography over a Source S column (AKTA FPLC). Labeling was performed in buffers containing 8M urea, hence the protein was completely denatured (evidenced by EPR spectra), and labeling efficiency was assumed to be nearly 100%. Protein concentrations were measured by the bicinchoninic acid (BCA) method using bovine serum albumin as the standard (BCA protein assay reagent; Pierce, Rockland, IL). All purified spin labeled proteins were stored long-term at  $-80^{\circ}\text{C}$ .

### ***In vitro* filament assembly and electron microscopy**

Protofilaments were generated by overnight dialysis against a Low Salt buffer (LS, 5 mM Tris-Cl, pH 7.5). Each mutant was examined by electron microscopy for the ability to form IFs *in vitro*; Supporting Information Figure 1 lists assembly results. In brief, protein at  $\sim 500$   $\mu\text{g}/\text{mL}$  in 8M urea was dialyzed overnight against intermediate filament assembly buffer (1 $\times$  IFAB (intermediate filament assembly buffer), 10 mM Tris-Cl, pH 7.5 and 160 mM NaCl) and approximately 10  $\mu\text{L}$  of the sample was removed, placed on formvar- and carbon-coated grids then stained with 1% uranyl acetate. Grids were imaged with a Phillips CM-120 electron microscope operated at 80 kV acceleration voltage.

### ***Electron paramagnetic resonance spectroscopy measurements***

EPR measurements of the site-directed spin labeled proteins were conducted on a JEOL X-band spectrometer equipped with a loop-gap resonator.<sup>18</sup> Samples were dialyzed against LS overnight and were induced to form IFs by the addition of 10 $\times$  assembly buffer (10 $\times$  IFAB). Immediately after addition of the assembly buffer, 6  $\mu\text{L}$  of sample was pipetted into the room temperature EPR capillary and spun in a low speed clinical centrifuge to collect assembling filaments at the bottom. Assembling filaments were also pipetted into the larger diameter low temperature capillaries and centrifuged. In a change from previous reports, we have begun using two low temperature capillaries in the resonator, increasing the signal to noise ratio.<sup>46</sup> Spectra of the samples were obtained by a single scan of 120 s over 100 G at a microwave power of 4 mW, at room temperature (unless otherwise specified). Modulation width (0.1–0.2 mT) was optimized to the natural line width of the attached nitroxide. Normalization of the spectra to the same number of spins was done by normalizing each spectrum to the same integrated

intensity.<sup>14,15</sup> To achieve improvement in the fidelity of the calculation, each sample was double integrated after its solubilization in 2%, sodium dodecyl sulfate which disrupts the coiled-coil association, thereby abolishing broadening due to dipolar interaction and/or strong spin-label immobilization due to tertiary/quaternary contacts.

### **Acknowledgments**

Technical assistance with electron microscopy was provided by G. Adamson of the Electron Microscopy Laboratory, Dept. of Medical Pathology and Laboratory Medicine, UC Davis School of Medicine.

### **References**

1. <http://www.interfil.org/>.
2. Omary MB (2009) "IF-pathies": a broad spectrum of intermediate filament-associated diseases. *J Clin Invest* 119:1756–1762.
3. Colucci-Guyon E, Portier MM, Dunia I, Paulin D, Pournin S, Babinet C (1994) Mice lacking vimentin develop and reproduce without an obvious phenotype. *Cell* 79: 679–694.
4. Muller M, Bhattacharya SS, Moore T, Prescott Q, Wedig T, Herrmann H, Magin TM (2009) Dominant cataract formation in association with a vimentin assembly disrupting mutation. *Hum Mol Genet* 18:1052–1057.
5. Geisler N, Weber K (1982) The amino acid sequence of chicken muscle desmin provides a common structural model for intermediate filament proteins. *EMBO J* 1: 1649–1656.
6. Geisler N, Kaufmann E, Weber K (1982) Proteinchemical characterization of three structurally distinct domains along the protofilament unit of desmin 10 nm filaments. *Cell* 30:277–286.
7. Hanukoglu I, Fuchs E (1982) The cDNA sequence of a human epidermal keratin: divergence of sequence but conservation of structure among intermediate filament proteins. *Cell* 31:243–252.
8. Hanukoglu I, Fuchs E (1983) The cDNA sequence of a Type II cytoskeletal keratin reveals constant and variable structural domains among keratins. *Cell* 33:915–924.
9. Herrmann H, Aebi U (2004) Intermediate filaments: molecular structure, assembly mechanism, and integration into functionally distinct intracellular scaffolds. *Annu Rev Biochem* 73:749–789.
10. Parry DA, Steinert PM (1999) Intermediate filaments: molecular architecture, assembly, dynamics and polymorphism. *Q Rev Biophys* 32:99–187.
11. Steinert PM, Parry DA (1985) Intermediate filaments: conformity and diversity of expression and structure. *Annu Rev Cell Biol* 1:41–65.
12. Goldman RD, Steinert PM (1990) Cellular and molecular biology of intermediate filaments. New York, NY: Plenum Press.
13. Herrmann H, Harris JR, Structure, assembly, and dynamics of Intermediate filaments, pp 319–362. In: *Intermediate Filaments*. Harris JR, Ed. (1998). New York, New York: Plenum.
14. Aziz A, Hess JF, Budamagunta MS, FitzGerald PG, Voss JC (2009) Head and rod 1 interactions in vimentin: identification of contact sites, structure, and changes with phosphorylation using site-directed spin labeling and electron paramagnetic resonance. *J Biol Chem* 284:7330–7338.



15. Aziz A, Hess JF, Budamagunta MS, Voss JC, FitzGerald PG (2010) Site-directed spin labeling and electron paramagnetic resonance determination of vimentin head domain structure. *J Biol Chem* 285:15278–15285.
16. Hess JF, Budamagunta MS, Shipman RL, FitzGerald PG, Voss JC (2006) Characterization of the linker 2 region in human vimentin using site-directed spin labeling and electron paramagnetic resonance. *Biochemistry* 45:11737–11743.
17. Hess JF, Budamagunta MS, Voss JC, Fitzgerald PG (2004) Structural characterization of human vimentin rod 1 and the sequencing of assembly steps in intermediate filament formation *in vitro* using site-directed spin labeling and electron paramagnetic resonance. *J Biol Chem* 279:44841–44846.
18. Hess JF, Voss JC, FitzGerald PG (2002) Real-time observation of coiled-coil domains and subunit assembly in intermediate filaments. *J Biol Chem* 277:35516–35522.
19. Nicolet S, Herrmann H, Aebi U, Strelkov SV (2010) Atomic structure of vimentin coil 2. *J Struct Biol* 170:369–376.
20. Strelkov S, Herrmann H, Parry D, Steinert P, Aebi U (YEAR) Atomic structure of the consensus motif of the 2B rod domain segment of the intermediate filament chain vimentin. *J Invest Dermatol* 1142000: 779.
21. Strelkov SV, Herrmann H, Geisler N, Wedig T, Zimbelmann R, Aebi U, Burkhard P (2002) Conserved segments 1A and 2B of the intermediate filament dimer: their atomic structures and role in filament assembly. *EMBO J* 21:1255–1266.
22. Strelkov SV, Kreplak L, Herrmann H, Aebi U (2004) Intermediate filament protein structure determination. *Methods Cell Biol* 78:25–43.
23. Herrmann H, Hofmann I, Franke WW (1992) Identification of a nonapeptide motif in the vimentin head domain involved in intermediate filament assembly. *J Mol Biol* 223:637–650.
24. Kouklis PD, Hatzfeld M, Brunkener M, Weber K, Georgatos SD (1993) *In vitro* assembly properties of vimentin mutagenized at the beta-site tail motif. *J Cell Sci* 106:919–928.
25. Kouklis PD, Papamarcaki T, Merdes A, Georgatos SD (1991) A potential role for the COOH-terminal domain in the lateral packing of type III intermediate filaments. *J Cell Biol* 114:773–786.
26. Hatzfeld M, Burba M (1994) Function of type I and type II keratin head domains: their role in dimer, tetramer and filament formation. *J Cell Sci* 107:1959–1972.
27. Rogers KR, Eckelt A, Nimmrich V, Janssen KP, Schliwa M, Herrmann H, Franke WW (1995) Truncation mutagenesis of the non-alpha-helical carboxyterminal tail domain of vimentin reveals contributions to cellular localization but not to filament assembly. *Eur J Cell Biol* 66:136–150.
28. Herrmann H, Häner M, Brettel M, Müller SA, Goldie KN, Fedtke B, Lustig A, Franke WW, Aebi U (1996) Structure and assembly properties of the intermediate filament protein vimentin: the role of its head, rod and tail domains. *J Mol Biol* 264:933–953.
29. Beuttenmuller M, Chen M, Janetzko A, Kuhn S, Traub P (1994) Structural elements of the amino-terminal head domain of vimentin essential for intermediate filament formation *in vivo* and *in vitro*. *Exper Cell Res* 213:128–142.
30. McCormick MB, Kouklis P, Syder A, Fuchs E (1993) The roles of the rod end and the tail in vimentin IF assembly and IF network formation. *J Cell Biol* 122:395–407.
31. Cary RB, Klymkowsky MW, Evans RM, Domingo A, Dent JA, Backhus LE (1994) Vimentin's tail interacts with actin-containing structures *in vivo*. *J Cell Sci* 107:1609–1622.
32. Mack JW, Torchia DA, Steinert PM (1988) Solid-state NMR studies of the dynamics and structure of mouse keratin intermediate filaments. *Biochemistry* 27:5418–5426.
33. Kaufmann E, Weber K, Geisler N (1985) Intermediate filament forming ability of desmin derivatives lacking either the amino-terminal 67 or the carboxy-terminal 27 residues. *J Mol Biol* 185:733–742.
34. Shoeman RL, Mothes E, Kesselmeier C, Traub P (1990) Intermediate filament assembly and stability *in vitro*: effect and implications of the removal of head and tail domains of vimentin by the human immunodeficiency virus type 1 protease. *Cell Biol Int Rep* 14:583–594.
35. Eckelt A, Herrmann H, Franke WW (1992) Assembly of a tail-less mutant of the intermediate filament protein, vimentin, *in vitro* and *in vivo*. *Eur J Cell Biol* 58:319–330.
36. Leonard DG, Gorham JD, Cole P, Greene LA, Ziff EB (1988) A nerve growth factor-regulated messenger RNA encodes a new intermediate filament protein. *J Biol Biol* 106:181–193.
37. Makarova I, Carpenter D, Khan S, Ip W (1994) A conserved region in the tail domain of vimentin is involved in its assembly into intermediate filaments. *Cell Motil Cytoskel* 28:265–277.
38. Der Perng M, Su M, Wen SF, Li R, Gibbon T, Prescott AR, Brenner M, Quinlan RA (2006) The Alexander disease-causing glial fibrillary acidic protein mutant, R416W, accumulates into Rosenthal fibers by a pathway that involves filament aggregation and the association of alpha B-crystallin and HSP27. *Am J Hum Genet* 79:197–213.
39. Mucke N, Wedig T, Burer A, Marekov LN, Steinert PM, Langowski J, Aebi U, Herrmann H (2004) Molecular and biophysical characterization of assembly-starter units of human vimentin. *J Mol Biol* 340:97–114.
40. Mchaurab H, Lietzow MA, Hideg K, Hubbell WL (1996) Motion of spin labeled side chains in T4 Lysozyme. (I) Correlation with protein structure and dynamics. *Biochemistry* 35:7692–7704.
41. Herrmann H, Strelkov SV, Feja B, Rogers KR, Brettel M, Lustig A, Häner M, Parry DA, Steinert PM, Burkhard P, Ueli Aebi. (2000) The intermediate filament protein consensus motif of helix 2B: its atomic structure and contribution to assembly. *J Mol Biol* 298:817–832.
42. Strelkov SV, Herrmann H, Geisler N, Lustig A, Ivaninskii S, Zimbelmann R, Burkhard P, Aebi U (2001) Divide-and-conquer crystallographic approach towards an atomic structure of intermediate filaments. *J Mol Biol* 306:773–781.
43. Aziz A, Hess JF, Budamagunta MS, Voss JC, Kuzin AP, Huang YJ, Xiao R, Montelione GT, Fitzgerald PG, Hunt JF (2012) The structure of vimentin linker 1 and rod 1B domains characterized by site-directed spin-labeling electron paramagnetic resonance (SDSL-EPR) and X-ray crystallography. *J Biol Chem* 287:28349–28361.
44. Kapinos LE, Burkhard P, Herrmann H, Aebi U, Strelkov SV (2011) Simultaneous formation of right- and left-handed anti-parallel coiled-coil interfaces by a coil2 fragment of human lamin A. *J Mol Biol* 408:135–146.
45. Eriksson JE, He T, Trejo-Skalli AV, Harmala-Brasken AS, Hellman J, Chou YH, Goldman RD (2004) Specific *in vivo* phosphorylation sites determine the assembly dynamics of vimentin intermediate filaments. *J Cell Sci* 117:919–932.
46. Nelson WD, Blakely SE, Nesselov YE, Thomas DD (2005) Site-directed spin labeling reveals a conformational switch in the phosphorylation domain of smooth muscle myosin. *Proc Natl Acad Sci USA* 102:4000–4005.